Communication: Determination of the bond dissociation energy (D_0) of the water dimer, $(H_2O)_2$, by velocity map imaging

Blithe E. Rocher-Casterline, Lee C. Ch'ng, Andrew K. Mollner,[a] and Hanna Reisler[b]
Department of Chemistry, University of Southern California, Los Angeles, California 90089-0482, USA

(Received 22 April 2011; accepted 18 May 2011; published online 1 June 2011)

The bond dissociation energy (D_0) of the water dimer is determined by using state-to-state vibrational predissociation measurements following excitation of the bound OH stretch fundamental of the donor unit of the dimer. Velocity map imaging and resonance-enhanced multiphoton ionization (REMPI) are used to determine pair-correlated product velocity and translational energy distributions. H_2O fragments are detected in the ground vibrational (000) and the first excited bending (010) states by 2 + 1 REMPI via the $\tilde{C}\ ^1B_1$ (000) $\leftarrow \tilde{X}\ ^1A_1$ (000 and 010) transitions. The fragments' velocity and center-of-mass translational energy distributions are determined from images of selected rovibrational levels of H_2O. An accurate value for D_0 is obtained by fitting both the structure in the images and the maximum velocity of the fragments. This value, $D_0 = 1105 \pm 10\ cm^{-1}$ (13.2 ± 0.12 kJ/mol), is in excellent agreement with the recent theoretical value of $D_0 = 1103 \pm 4\ cm^{-1}$ (13.2 ± 0.05 kJ/mol) suggested as a benchmark by Shank *et al.* [J. Chem. Phys. **130**, 144314 (2009)]. © *2011 American Institute of Physics*. [doi:10.1063/1.3598339]

The water dimer is the smallest water cluster and, as such, much scientific effort has been directed toward understanding its properties. Surprisingly, despite experimental work on the structure, spectroscopy, bond rearrangements, and tunneling dynamics of the dimer,[1–25] there is no direct measurement of its dissociation energy (D_0). In contrast, detailed theoretical work has been devoted to the electronic structure of the dimer, including its interaction energy (D_e) and zero point energy (ZPE), which are needed to determine D_0.[22,26–38] In addition to serving as a benchmark for theory, an accurate experimental value of D_0 is important for evaluating the dimer's absorption in the atmosphere.[36]

The equilibrium structure of the H_2O-H_2O dimer has been determined experimentally[1,2] and theoretically.[29,37] The hydrogen bond is nearly linear and the structure is floppy. Tunneling motions and their barriers also have been studied.[3,4,39] IR spectra of the water dimer have been measured in low-temperature matrices,[7–12] He droplets,[13] and (in high resolution) the gas phase.[14,15] The bound OH stretch was initially assigned as the vibrational band near 3532 cm^{-1},[14] but later reassigned to the 3601 cm^{-1} band.[16,17] This band is only partially rotationally resolved due to predissociation, and the lifetime is estimated to be 80 ps.[15]

Several recent calculations of D_0 of $(H_2O)_2$ have been reported.[22,27–33] These values appear to converge around 1100 cm^{-1} with a spread of about 100 cm^{-1}. In these studies, D_e and ZPE are used to determine D_0. Advances in electronic structure methods enabled precise calculation of ZPE at the coupled-cluster single double triple (CCSD(T)) level of theory and, in turn, D_0.[29,30,32] Most recently, Shank *et al.* utilized a modified full-dimensional potential energy surface with CCSD(T)/aug-ccpVTZ level of theory/basis set and diffusion Monte Carlo calculations to determine $D_0 = 1103 \pm 4$ cm^{-1} for the H_2O-H_2O dimer.[30] This benchmark value awaits experimental verification.

So far, only indirect experimental methods have been used to estimate the binding energy of $(H_2O)_2$.[18–24] These measurements were done at temperatures 270–723 K and gave the enthalpy of dimerization, ΔH^o, rather than D_0. The experimental values are spread over a broad range (1133–1819 cm^{-1}; 13.6–21.8 kJ/mol) and have large error bars. Extracting the value of D_0 from these experiments is complicated due to the indirect nature of the measurements and the difficulty of estimating the thermal contributions (including vibrational, rotational, translational, and pressure and temperature effects).[22,29,40] We report here the first measurement of D_0 of the H_2O-H_2O dimer at low temperature that can be directly compared to theory.

Recently, we have used velocity map imaging (VMI) to obtain accurate values of D_0 for several hydrogen-bonded dimers.[41–46] In this method, isolated rovibrational levels of a fragment are monitored following IR vibrational predissociation (VP) of the dimer, and photofragment images are recorded. From the structured velocity and center-of-mass (c.m.) translational energy (E_T) distributions, pair-correlated energy distributions of the cofragment are obtained. Fitting the structural features and maxima in the velocity distributions in several such images gave unique and accurate values of D_0 for the dimers with an accuracy of $\pm 10\ cm^{-1}$. Our work on the H_2O-HCl dimer[41,42] is most relevant to the present study, being a first case in which the water fragment was monitored directly by resonance-enhanced multiphoton ionization (REMPI).[42] From images obtained by monitoring selected rotational levels of *either* HCl or H_2O fragments $D_0 = 1334 \pm 10\ cm^{-1}$ was obtained.

[a] Present address: The Aerospace Corporation, 2310 E. El Segundo Blvd., El Segundo, California 90245, USA
[b] Author to whom correspondence should be addressed. Electronic mail: reisler@usc.edu. Tel.: 213-740-7071. Fax: 213-740-3972.

In this Communication, we report the first determination of D_0 for the water dimer in a supersonic molecular beam. The key to our success is our ability to obtain REMPI spectra of water fragments. Following excitation of the bound OH stretch of the dimer, images are obtained by monitoring selected H_2O fragment rotational levels, J''_{KaKc}, in the ground (000) and the first excited bending (010) states. The experimental procedures were similar to those used in our previous studies.[41–46]

Dimers were formed in a pulsed supersonic molecular beam by expanding a mixture of ~2% H_2O in He at a stagnation pressure of ~1.5 atm through the 0.5-mm orifice of a pulsed valve. The rotational temperature of the dimer was estimated to be 10 ± 5 K.[41,43] Focused IR laser radiation [~2–12 mJ/pulse, lens focal length (f.l.) = 20 cm, 0.4 cm^{-1} linewidth] was used to excite the bound OH stretch of the dimer, and focused ultraviolet (UV) radiation (247–254 nm; 0.2–1.1 mJ/pulse, f.l. = 20 cm; ~0.4 cm^{-1} linewidth) ionized state-selected H_2O fragments. The UV beam was expanded by using an additional lens (f.l. = −100 cm) placed 137 cm before the focusing lens.[42] The $\tilde{C}\ ^1B_1$ (000) ← $\tilde{X}\ ^1A_1$ (000 and 010) bands were used for H_2O REMPI detection and modeled using the PGOPHER program with rotational constants from Yang *et al.*[42,47] Spectra were collected by alternating "IR on" and "IR off" conditions at each frequency. Laser conditions (timing, focusing, power) were optimized to maximize signal from the dimer.

Two modes were used to collect data: (i) TOF mass spectrometry for spectroscopic investigations and (ii) VMI mode for determining c.m. translational energy distributions. The VMI arrangement was described previously.[48,49] Two-dimensional projections were collected using event counting and reconstructed using the BASEX method.[50] Velocity distributions were obtained by summing over the angular distribution for each radius and were converted to c.m. translational energy distributions in the usual way.[41–45] Calibration was achieved by imaging NO products from NO_2 photodissociation.[51]

Infrared spectrum of $(H_2O)_2$. IR spectra of the dimer excited to the bound OH stretch fundamental were recorded by monitoring H_2O photofragments in selected rovibrational states by REMPI while scanning the IR laser frequency. A typical spectrum obtained by monitoring H_2O (010) $J''_{KaKc} = 3_{21}$ is shown in Fig. 1. No contributions from other H_2O containing clusters were seen in the region of the dimer peak (3530–3630 cm^{-1}).[13–15] The spectrum exhibits saturation broadening due to the tight focusing of the IR radiation necessary to maximize signals from H_2O fragments. For REMPI and ion imaging, our IR frequency was set to 3602 cm^{-1}, where dimers in the range $J'' = 2$ and 3, and $K_a = 0$ and 1 were likely excited.[52] This gives an average internal energy $E_{int}(H_2O\text{-}H_2O) = 5 \pm 5\ cm^{-1}$.

REMPI spectroscopy of H_2O fragments. Representative REMPI spectra of H_2O fragments in the region of the $\tilde{C}\ ^1B_1$ (000) ← $\tilde{X}\ ^1A_1$ (000 and 010) bands are shown in Fig. 2. The spectra show enhancement (relative to the IR off signal) for several isolated rotational states that can be used for imaging. A 250 K simulation obtained by using the PGOPHER program (Ref. 53) is shown for comparison of line positions.

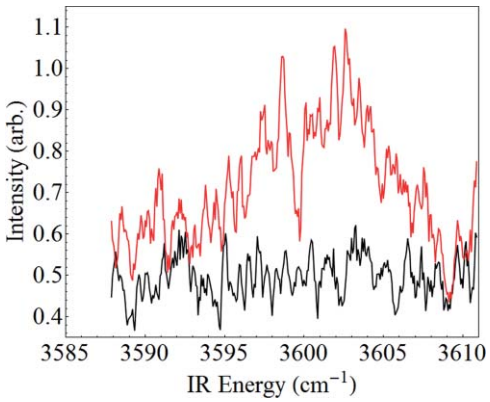

FIG. 1. IR spectrum of $(H_2O)_2$ recorded by monitoring H_2O ($J''_{KaKc} = 3_{21}$) fragments via the $\tilde{C}\ ^1B_1$ (000) ← $\tilde{X}\ ^1A_1$ (010) transition. The IR laser energy was 10 mJ/pulse (f.l. = 20 cm). The red (top) curve shows the enhancement signal from the dimer and the black (bottom) curve shows the background signal under the same conditions.

In spite of fast predissociation in the $\tilde{C}$-state and spectral congestion,[42] several isolated transitions of water fragments could be used for imaging. The detection of water fragments in the ground (000) level was reported previously,[42,47] and because the available energy allowed formation of water fragments in the (010) bending state, we detected it via the $\tilde{C}\ ^1B_1$ (000) ← $\tilde{X}\ ^1A_1$ (010) transition. Although no prior description of this transition was published, it was well simulated by the PGOPHER program.[53,54]

Ion imaging results and analysis. Representative velocity spectra obtained by VMI of selected H_2O (J''_{KaKc}) levels in the (000) and (010) vibrational states are shown in Figs. 3 and 4. The angular distributions of all of the images were isotropic.

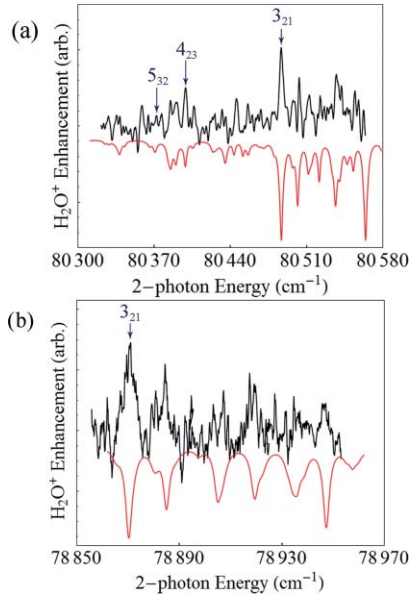

FIG. 2. The black (top) curves correspond to the H_2O photofragment 2+1 REMPI enhancement spectrum obtained by exciting the bound OH stretch of $(H_2O)_2$ at 3602 cm^{-1} and scanning the UV laser through the region of the (a) $\tilde{C}\ ^1B_1$ (000) ← $\tilde{X}\ ^1A_1$ (000) and (b) $\tilde{C}\ ^1B_1$ (000) ← $\tilde{X}\ ^1A_1$ (010) transitions of H_2O. The inverted red (bottom) curves correspond to simulated spectra at $T = 250$ K. Both the IR and UV laser powers were held constant over the range of the scan. The H_2O (J''_{KaKc}) rotational levels used to obtain the images shown in Figs. 3 and 4 are labeled.

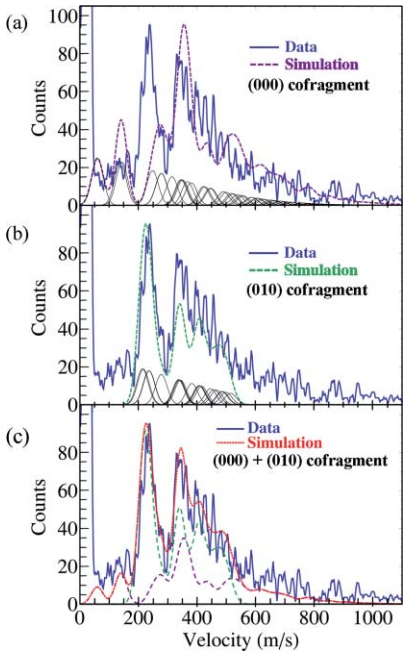

FIG. 3. Velocity distribution from a reconstructed image obtained by monitoring H_2O ($J''_{KaKc} = 5_{32}$) fragments (velocity in m/s = 5.2 × pixels). Positions of the Gaussians used in the simulations were determined by using D_0 as a fit parameter and the known $H_2O(J''_{KaKc})$ rotational energies corresponding to the cofragments in (a) (000) and (b) (010) states. Simulations for (000) and (010) states were combined in a 0.5:1 ratio to give the best fit shown in (c).

Conservation of energy requires,

$$E_{\text{int}}(\text{H}_2\text{O-H}_2\text{O}) + h\nu = D_0 + E_{\text{T}} + E_{\text{vib}}(\text{H}_2\text{O}) + E_{\text{rot}}(\text{H}_2\text{O}) + E_{\text{vib}}(\text{H}_2\text{O}^{\text{cofrag}}) + E_{\text{rot}}(\text{H}_2\text{O}^{\text{cofrag}}), \quad (1)$$

where $E_{\text{int}}(\text{H}_2\text{O-H}_2\text{O})$ is the internal energy of the dimer, estimated to be 5 cm^{-1} (see above); $h\nu$ = 3602 cm^{-1}, and $E_{\text{rot (vib)}}(\text{H}_2\text{O})$ and $E_{\text{rot(vib)}}(\text{H}_2\text{O}^{\text{cofrag}})$ are the rotational and vibrational energies of each H_2O fragment. The velocity and E_T distributions are determined from the images. State selective REMPI defines $E_{\text{vib}}(\text{H}_2\text{O})$ and $E_{\text{rot}}(\text{H}_2\text{O})$ of one fragment, while the energy of the cofragment, $E_{\text{vib}}(\text{H}_2\text{O}^{\text{cofrag}})$ and $E_{\text{rot}}(\text{H}_2\text{O}^{\text{cofrag}})$, as well as D_0 are determined from fits of the reconstructed images.

Reconstructed images in velocity space were used to determine the rotational states of the pair-correlated water-fragments. Fitting was accomplished, as described before,[41–46] by assigning a Gaussian-shaped curve to each rotational state of H_2O,[55] with a width characteristic of the experimental resolution (~8 pixels or 44 m/s). This width was obtained from images of H_2O (J''_{KaKc}) levels from VP of HCl-H_2O, where rotational levels of the HCl cofragment were resolved.[42] The positions of the Gaussians were then shifted together by adjusting D_0 until *both* the observed structure and maximum velocity were well matched in all the images. Since our goal was to determine D_0 rather than product state distributions, the heights of the Gaussians were described by an exponentially decaying function of E_T, corresponding to an increase in rotational population with decreasing E_T. All images had clearly discernible structures that could be fit with a consistent and unique D_0. Images were collected by monitoring isolated transitions from the $\tilde{X}^1A_1$ (000) and (010) states, and from fits of eight images, D_0 of 1100 ± 3 cm^{-1} (2σ) was derived, assuming no uncertainty in other parameters (see below).

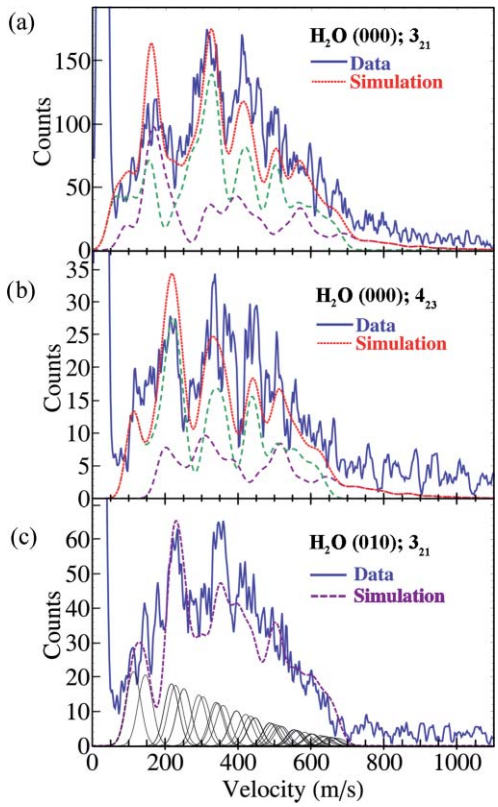

FIG. 4. Velocity distributions from reconstructed images obtained by monitoring state-selected H_2O fragments (velocity in m/s = 5.2 × pixels). The images were recorded while monitoring (a) H_2O [(000) $J''_{KaKc} = 3_{21}$], (b) H_2O [(000) $J''_{KaKc} = 4_{23}$], and (c) H_2O [(010) $J''_{KaKc} = 3_{21}$]. In (a) and (b) the structural features in the spectra are best fit (red) with a combination of cofragments in (000) (green) and (010) (purple) states. See the text for details.

For images recorded while monitoring fragments in the (000) state, J''_{KaKc} levels of cofragments in *both* the ground (000) and excited bending (010) states were needed for best fits, as shown in Fig. 3. Whereas the major structural features were fit well by assuming that the cofragment is in the (010) state, the regions of high and low velocities were fit better by including the ground (000) rotational levels as well. The simulations use a (000):(010) = 0.5:1 ratio, which seems to fit the structure well in all the images. Images recorded while monitoring fragments in the (010) state [Fig. 4(c)], which can have cofragments only in the (000) state, were fit well with the same value of D_0.

Dissociation energy of the H_2O-H_2O dimer. Several factors lend confidence to the accuracy of the D_0 value reported here. Most important is the consistency of D_0 required to fit all the images obtained by monitoring different rovibrational states of H_2O. All images were fit with D_0 within a range of ±4 cm^{-1}, which is narrowly constrained by the specific structure in the velocity distributions. The finite width of the observed peaks places a lower limit on our fitting uncertainty at ±2 cm^{-1}, but depending on the signal-to-noise ratio the uncertainty in a specific image can be as high as ±8 cm^{-1}. However, the need to fit *all* the images with the same D_0 value

restricts the acceptable values. The uncertainty in the IR frequency is on the order of 1 cm^{-1} and in the internal energy of the dimer is ± 5 cm^{-1}. Combining uncertainties, we arrive at $D_0 = 1105 \pm 10$ cm^{-1}.

Several attempts have been made to determine the binding energy of $(H_2O)_2$ experimentally but they were carried out at higher temperatures (270–723 K) and gave ΔH^o indirectly.[18–24] These methods include the increase in thermal conductivity upon dimerization ($T = 358$–386 K; $\Delta H^\circ = 15.02 \pm 2.10$ kJ/mol),[19] and measurements of integrated IR absorption ($T = 573$–723 K; $\Delta H^\circ = 16.65 \pm 3.77$ kJ/mol,[24] and $T = 373$–673 K; $\Delta H^\circ = 15 \pm 3$ kJ/mol).[21] In addition, the pressure broadening of water vapor was investigated using cavity ring-down spectroscopy at room temperature, and the water dimer binding energy was estimated from the water-rare gas interaction energies.[21,22,40] The derived values were 13.6 ± 4 kJ/mol (Refs. 22 and 40) and 15.5 ± 5.6 kJ/mol.[23] Though the values determined using these methods are valuable in estimating the feasibility of detecting the water dimer in the atmosphere,[36] they cannot be directly compared to our value of D_0, as described above. However, within the range of their error bars, they appear to be in good agreement with our value of $D_0 = 13.2 \pm 0.05$ kJ/mol.

The recent high-level electronic structure calculations are capable of determining D_e accurately.[22,27–33] To obtain D_0 from the calculated D_e the difference between the ZPE's of the dimer and the monomer fragments needs to be evaluated as well. The most recent high-level calculations by Shank *et al.*[30] give $D_0 = 1103$ cm^{-1} (13.2 kJ/mol) at the CCSDT(T)/aug-ccpVTZ level of theory/basis set with the addition of several modifications to the potential energy surface. This value, which is proposed as a benchmark for theory, matches our experimental value of $D_0 = 1105 \pm 10$ cm^{-1} (13.2 ± 0.12 kJ/mol) very well.

This material is based upon work supported by the National Science Foundation under Grant No. CHE-0951976. The authors thank Professor Colin Western for assistance with simulating the water REMPI spectra, Dr. Amit Samanta for helpful discussions and Professor Joel Bowman whose theoretical work inspired the current measurements.

[1] L. H. Coudert and J. T. Hougen, J. Mol. Spectrosc. **139**, 259 (1990).
[2] J. A. Odutola and T. R. Dyke, J. Chem. Phys. **72**, 5062 (1980).
[3] L. B. Braly, K. Liu, M. G. Brown, F. N. Keutsch, R. S. Fellers, and R. J. Saykally, J. Chem. Phys. **112**, 10314 (2000).
[4] N. Pugliano, J. D. Cruzan, J. G. Loeser, and R. J. Saykally, J. Chem. Phys. **98**, 6600 (1993).
[5] J. B. Paul, C. P. Collier, R. J. Saykally, J. J. Scherer, and A. Okeefe, J. Phys. Chem. A **101**, 5211 (1997).
[6] N. Goldman, R. S. Fellers, M. G. Brown, L. B. Braly, C. J. Keoshian, C. Leforestier, and R. J. Saykally, J. Chem. Phys. **116**, 10148 (2002).
[7] Y. Bouteiller and J. P. Perchard, Chem. Phys. **305**, 1 (2004).
[8] J. P. Perchard, Chem. Phys. **273**, 217 (2001).
[9] J. P. Perchard, Chem. Phys. **266**, 109 (2001).
[10] J. Ceponkus, P. Uvdal, and B. Nelander, J. Phys. Chem. A **112**, 3921 (2008).
[11] J. Ceponkus and B. Nelander, J. Phys. Chem. A **108**, 6499 (2004).
[12] S. Coussan, P. Roubin, and J. P. Perchard, Chem. Phys. **324**, 527 (2006).
[13] K. Kuyanov-Prozument, M. Y. Choi, and A. F. Vilesov, J. Chem. Phys. **132**, 014304 (2010).
[14] Z. S. Huang and R. E. Miller, J. Chem. Phys. **91**, 6613 (1989).
[15] J. B. Paul, R. A. Provencal, C. Chapo, A. Petterson, and R. J. Saykally, J. Chem. Phys. **109**, 10201 (1998).
[16] F. Huisken, M. Kaloudis, and A. Kulcke, J. Chem. Phys. **104**, 17 (1996).
[17] U. Buck and F. Huisken, Chem. Rev. **100**, 3863 (2000).
[18] H. A. Gebbie, W. J. Burrough, J. Chamberlain, J. E. Harries, and R. G. Jones, Nature (London) **221**, 143 (1969).
[19] L. A. Curtiss, D. J. Frurip, and M. Blander, J. Chem. Phys. **71**, 2703 (1979).
[20] V. I. Dianov-Klokov, V. M. Ivanov, V. N. Arefev, and N. I. Sizov, J. Quant. Spectrosc. Radiat. Transf. **25**, 83 (1981).
[21] Y. Jin and S. Ikawa, J. Chem. Phys. **119**, 12432 (2003).
[22] T. Nakayama, H. Fukuda, T. Kamikawa, Y. Sakamoto, A. Sugita, M. Kawasaki, T. Amano, H. Sato, S. Sakaki, I. Morino, and G. Inoue, J. Chem. Phys. **127**, 134302 (2007).
[23] P. A. Y. Fiadzomor, A. M. Keen, R. B. Grant, and A. J. Orr-Ewing, Chem. Phys. Lett. **462**, 188 (2008).
[24] G. V. Bondarenko and Y. E. Gorbaty, Mol. Phys. **74**, 639 (1991).
[25] S. A. Nizkorodov, M. Ziemkiewicz, D. J. Nesbitt, and A. E. W. Knight, J. Chem. Phys. **122**, 194316 (2005).
[26] J. R. Lane and H. G. Kjaergaard, J. Chem. Phys. **131**, 034307 (2009).
[27] C. Leforestier, R. van Harrevelt, and A. van der Avoird, J. Phys. Chem. A **113**, 12285 (2009).
[28] J. K. Gregory and D. C. Clary, J. Phys. Chem. **100**, 18014 (1996).
[29] W. Klopper, J. G. C. M. van Duijneveldt-van de Rijdt, and F. B. van Duijneveldt, Phys. Chem. Chem. Phys. **2**, 2227 (2000).
[30] A. Shank, Y. Wang, A. Kaledin, B. J. Braams, and J. M. Bowman, J. Chem. Phys. **130**, 144314 (2009).
[31] N. Goldman and R. J. Saykally, J. Chem. Phys. **120**, 4777 (2004).
[32] X. Huang, B. J. Braams, and J. M. Bowman, J. Phys. Chem. A **110**, 445 (2006).
[33] G. C. Groenenboom, P. E. S. Wormer, A. van der Avoird, E. M. Mas, R. Bukowski, and K. Szalewicz, J. Chem. Phys. **113**, 6702 (2000).
[34] X. Huang, B. J. Braams, J. M. Bowman, R. E. A. Kelly, J. Tennyson, G. C. Groenenboom, and A. van der Avoird, J. Chem. Phys. **128**, 034312 (2008).
[35] H. G. Kjaergaard, A. L. Garden, G. M. Chaban, R. B. Gerber, D. A. Matthews, and J. F. Stanton, J. Phys. Chem. A **112**, 4324 (2008), and references therein.
[36] N. Goldman, C. Leforestier, and R. J. Saykally, J. Phys. Chem. A **108**, 787 (2004).
[37] K. S. Kim, B. J. Mhin, U. S. Choi, and K. Lee, J. Chem. Phys. **97**, 6649 (1992), and references therein.
[38] G. C. Groenenboom, E. M. Mas, R. Bukowski, K. Szalewicz, P. E. S. Wormer, and A. van der Avoird, Phys. Rev. Lett. **84**, 4072 (2000).
[39] L. B. Braly, K. Liu, M. G. Brown, F. N. Keutsch, R. S. Fellers, and R. J. Saykally, J. Chem. Phys. **112**, 10314 (2000).
[40] H. Sato, S. Sakaki, Y. Sakamoto, and M. Kawasaki, Chem. Lett. **39**, 296 (2010).
[41] B. E. Casterline, A. K. Mollner, L. C. Ch'ng, and H. Reisler, J. Phys. Chem. A **114**, 9774 (2010).
[42] B. E. Rocher-Casterline, A. K. Mollner, L. C. Ch'ng, and H. Reisler, J. Phys. Chem. A (in press).
[43] A. K. Mollner, B. E. Casterline, L. C. Ch'ng, and H. Reisler, J. Phys. Chem. A **113**, 10174 (2009).
[44] G. Li, J. Parr, I. Fedorov, and H. Reisler, Phys. Chem. Chem. Phys. **8**, 2915 (2006).
[45] J. A. Parr, G. Li, I. Fedorov, A. J. McCaffery, and H. Reisler, J. Phys. Chem. A **111**, 7589 (2007).
[46] M. Pritchard, J. Parr, G. Li, H. Reisler, and A. McCaffery, Phys. Chem. Chem. Phys. **9**, 6241 (2007).
[47] C.-H. Yang, G. Sarma, J. J. ter Meulen, D. H. Parker, and C. M. Western, Phys. Chem. Chem. Phys. **12**, 13983 (2010).
[48] A. T. J. B. Eppink and D. H. Parker, Rev. Sci. Instrum. **68**, 3477 (1997).
[49] V. Dribinski, A. B. Potter, I. Fedorov, and H. Reisler, J. Chem. Phys. **121**, 12353 (2004).
[50] V. Dribinski, A. Ossadtchi, V. A. Mandelshtam, and H. Reisler, Rev. Sci. Instrum. **73**, 2634 (2002).
[51] A. V. Demyanenko, V. Dribinski, H. Reisler, H. Meyer, and C. X. W. Qian, J. Chem. Phys. **111**, 7383 (1999).
[52] R. E. A. Kelly, J. Tennyson, G. C. Groenenboom, and A. van der Avoird, J. Quant. Spectrosc. Radiat. Transf. **111**, 1262 (2010), and references therein.
[53] C. M. Western, pgopher, a program for simulating rotational structure, University of Bristol, 2011; see http://pgopher.chm.bris.ac.uk.
[54] C. M. Western, personal communication (2011).
[55] J. Tennyson, N. F. Zobov, R. Williamson, O. L. Polyansky, and P. F. Bernath, J. Phys. Chem. Ref. Data **30**, 735 (2001).